FEBS Letters 493 (2001) 122–128 FEBS 24721

Annexin A5 D226K structure and dynamics: identification of a molecular switch for the large-scale conformational change of domain III

Jana Sopkova-De Oliveira Santos[a], Michel Vincent[b], Sébastien Tabaries[c], Anne Chevalier[c], Daniel Kerbœuf[c], Françoise Russo-Marie[c], Anita Lewit-Bentley[b], Jacques Gallay[b,*]

[a] *UFR des Sciences Pharmaceutiques, 5 rue Vaubenard, F-14032 Caen, France*
[b] *L.U.R.E. Laboratoire pour l'Utilisation du Rayonnement Electromagnétique, Université Paris-Sud, Bâtiment 209D, P.O. Box 34, F-91898 Orsay Cedex, France*
[c] *I.C.G.M. U332 INSERM Hôpital Cochin, 22 rue Méchin, F-75014 Paris, France*

Received 9 February 2001; accepted 28 February 2001

First published online 14 March 2001

Edited by Hans Eklund

Abstract The domain III of annexin 5 undergoes a Ca^{2+}- and a pH-dependent conformational transition of large amplitude. Modeling of the transition pathway by computer simulations suggested that the interactions between D226 and T229 in the IIID–IIIE loop on the one hand and the H-bond interactions between W187 and T224 on the other hand, are important in this process [Sopkova et al. (2000) Biochemistry 39, 14065–14074]. In agreement with the modeling, we demonstrate in this work that the D226K mutation behaves as a molecular switch of the pH- and Ca^{2+}-mediated conformational transition. In contrast, the hydrogen bonds between W187 and T224 seem marginal.

Key words: Annexin 5; Calcium- and pH-induced conformational change; Electrostatic interaction; X-ray diffraction; Time-resolved fluorescence; Tryptophan

1. Introduction

Annexin 5 belongs to a family of water-soluble proteins widely distributed in different species, tissues, and cell types where they represent up to 1% of the total cell proteins. They share large functional and structural homologies [1]. Their exact function remains to be precisely determined, though they play a role in several physiological functions involving membrane trafficking [1–3]. They are involved in membrane fusion processes occurring in endo- and exocytosis, in anti-inflammatory and anti-coagulant phenomena in vitro [1] or ion channel activity [2] and in oxidative stress [4]. These different functions involve a common molecular step, which is the reversible Ca^{2+}-mediated binding of these proteins to the surface of negatively charged phospholipid membranes [5]. This interaction provokes large conformational changes particularly of domain III, affecting the single tryptophan residue of annexin A5 (Anx5) [6–13]. The binding of Ca^{2+} alone also induces a similar large-scale conformational transition of domain III [9,14–17]. The comparison of the Anx5 structures with and without bound Ca^{2+} in domain III shows that the unique tryptophan of the protein (W187) in the IIIA–IIIB loop moves from a buried position in the absence of calcium ('closed' A-form) onto the surface of the protein when the calcium ion is bound ('open' B-form) [14,15]. The Ca^{2+}-triggered conformational transition in the absence of membranes occurs at higher Ca^{2+} concentrations than in their presence. Mild-acidic pH conditions ($6 \geq pH \geq 4$) [18,19] can mimic this Ca^{2+}-induced conformational change of domain III. Moreover, the same conformational change is observed in the absence of calcium upon incorporation of Anx5 into reverse micelles [13], a membrane/water-interface-mimicking system, within which the apparent pH is lower than in bulk water [20]. These results suggest that specific electrostatic interactions could be crucial for the conformation of domain III.

Computer simulations of the pathway of the Ca^{2+}-mediated conformational transition of domain III carried out recently, pointed out the importance of this type of interactions, involving in particular residue aspartic acid 226 (D226) [21]. The examination of the crystal structures of the 'closed' A-form [15,22] and of the 'open' B-form [14,15] shows that the D226 carboxylic side-chain is involved in a hydrogen-bridge with the hydroxyl group of T229 side-chain, which may take a part in stabilizing the IIID–IIIE loop in the 'closed' A-form (Fig. 1). In Anx3, whose domain III is in the 'open' A-form in the absence of bound calcium [23], the position equivalent to D226 is occupied by a lysine residue (K229) and that of T229 by L232, which suppresses this interaction. Besides other amino acid changes, this suppression could partly explain the differences of conformation of these two highly homologous proteins. In addition to these interactions, the simulations suggested that the tryptophan residue itself could also play a role in the stabilization of the A-form, where the indole ring is involved in hydrogen-bond interactions with the side-chain of threonine 224 (T224) [21].

In order to provide experimental support to the importance of the interactions proposed by the model, two single point mutants of Anx5 were constructed: D226K and T224V. These mutants were studied by X-ray crystallography and fluorescence spectroscopy of the W187 residue. The results show that the single point mutation D226K is sufficient to provoke the large-scale conformational transition of domain III. In contrast, the suppression of the hydrogen bond between the in-

*Corresponding author. Fax: (33)-1-64468082.
E-mail: gallay@lure.u-psud.fr

Abbreviations: Anx5, annexin A5; W187, tryptophan 187; T224, threonine 224; D226, aspartic acid 226; D226K, mutant of human annexin V where aspartic 226 is replaced by a lysine; T224V, mutant of human annexin V where threonine 224 is replaced by a valine; MEM, maximum entropy method

0014-5793/01/$20.00
PII: S0014-5793(01)02285-2

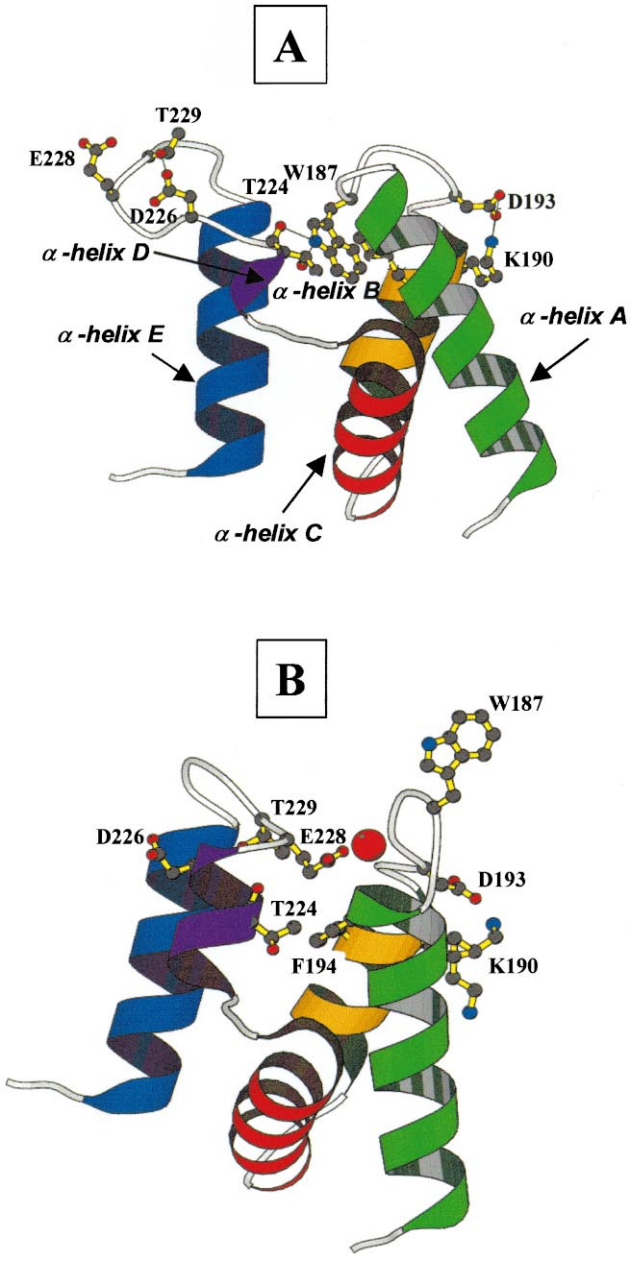

Fig. 1. Ribbon representation of the three-dimensional structure of domain III of annexin 5. A: 'closed' A-form without Ca^{2+} bound in domain III. B: 'open' B-form with bound Ca^{2+}. The five α-helices are represented in different colors and are indicated in A. Amino acid side-chains of W187, D190, K193, F194, T224, D226, E228 and T229 are represented as balls-and-sticks. Figure made using Molscript [48].

dole ring and the T224 hydroxyl group by the point mutation T224V, while increasing the W187 mobility with respect to the Anx5 wild-type, does not induce the large-scale conformational change.

2. Materials and methods

2.1. Chemicals

Phospholipids (1-2-dioleoyl-*sn*-glycerophosphocholine, DOPC, and 1-palmitoyl-2-oleoyl-*sn*-glycerophosphoserine, POPS) were obtained from Avanti polar lipids. All other chemicals were of the highest grade commercially available.

2.2. Protein preparation

Recombinant human Anx5 was prepared as before [24]. Mutagenesis of annexin V was performed directly onto the pGex-anx5 vector using the Quickchange site mutagenesis protocol from Stratagene. Briefly, 25 ng of the DNA template was mixed with 10 mM dNTP, 140 ng of oligonucleotide primer D226Kupper (5′-GGATTTCAAATTGAGGAAACCATTAAGCGCGAGACTTCTGGC-3′), 140 ng of oligonucleotide primer D226Klower (5′-GCCAGAAGTCTCGCGCTTAATGGTTTCCTCAATTTGAAATCC-3′) and 2.5 units of *Pfu* DNA polymerase. The mutated plasmid was synthesized and amplified by 16 cycles of 30 s at 95°C, 1 min at 55°C and 12 min at 68°C, followed by a 1-h treatment at 37°C in the presence of 5 units of *Dpn*I. Xl1blue competent cells were transformed by electroporation with 1 μl of the *Dpn*I-treated DNA. The mutations were checked by DNA sequencing.

During the preparation procedures and storage of the wild-type annexin V and of its mutants, calcium is removed by addition of EDTA. For measurements of absorbance and fluorescence, the protein solutions were prepared in the following buffers at 50 mM concentration: sodium acetate for pH 4, Tris–HCl for pH 7.5.

2.3. X-ray structure determination

Crystals of D226K mutant were obtained by a combination of vapor diffusion and micro-seeding, using ammonium sulfate as a precipitant. The first drop of 1.8 μl containing 11 mg ml^{-1} protein, 5 mM $CaCl_2$ and 1.1 M ammonium sulfate in 50 mM Tris–HCl buffer at pH 8, was equilibrated against a well containing 2 M ammonium sulfate in the same buffer. The first twinned crystal appeared after 3 days. This crystal was broken and dissolved to prepare the seeding solution. The second drop of 1.8 μl, containing a lower initial concentration of ammonium sulfate (11 mg ml^{-1} of protein, 5 mM $CaCl_2$ and 1 M ammonium sulfate in 50 mM Tris–HCl buffer at pH 8), to which 0.2 μl from the seeding solution was added, was equilibrated against a well containing 1.8 M ammonium sulfate in the same buffer. Single crystals grew in 3 weeks. The crystals were rhombohedric, space group R3, with cell dimensions $a = 158.53$ Å, $b = 158.53$ Å, $c = 36.74$ Å, $\gamma = 120°$ and with one molecule per asymmetric unit, isomorphous to other crystals of Anx5 [14,25].

Data were collected on the DW32 station on the DCI synchrotron ring at LURE, Orsay, France, equipped with an image plate detector (MARresearch), using a wavelength of 0.97 Å and a crystal-to-detector distance of 180 mm. The data reduction was performed using DENZO and the CCP4 program suite [26]. The crystal data characteristics are summarized in Table 1. Since the crystals of the D226K mutant are isomorphous to those of the E78Q human annexin V mutant, its coordinates from the Protein Data Bank (PDB code 1HVG) [25] were used directly as a starting model. This model was initially refined with a few cycles of the restrained automated refinement procedure (ARP) [27], followed by several rounds of alternate manual reconstruction on a graphics terminal with O [28] and refine-

Table 1
Model refinement statistics of Anx5 D226K

Parameters	
Resolution (Å)	10–2.3
Number of reflection used for refinement	15270
Number of	
Non-hydrogen protein atoms	2479
Calcium ions	1
Sulfate ions	1
Solvent molecules	118
R-factor (%)[a]	19.4
R_{free} (%)[b]	26.3
Mean B-factor	
Protein atoms (Å^2)	34.62
Solvent molecules (Å^2)	40.75
rms deviation from target values	
Bonds (Å)	0.016
Planes (Å)	0.014
Torsion (°)	2.1

[a] $R = (\Sigma|F_o - F_c|/\Sigma F_o)$ where F_o and F_c are the observed and calculated structure factor respectively.
[b] R_{free} is defined in [47]; 10% exclusion was used.

ment by REFMAC [29]. Table 1 summarizes the characteristics of the final model.

2.4. Steady-state and time-resolved fluorescence measurements

Tryptophan fluorescence emission spectra were recorded on a SLM 8000 spectrofluorometer equipped with Hamamatsu photon counting detectors (model H3460-53) at an excitation wavelength of 295 nm. The protein concentration was ~10 μM. To remove polarization artifacts, the fluorescence emission spectra were reconstructed from the four polarized spectra [30].

Fluorescence intensity and anisotropy decays were obtained by the time-correlated single photon counting technique from the $I_{vv}(t)$ and $I_{vh}(t)$ components recorded on the experimental set-up installed on the SB1 station on the synchrotron radiation source Super-ACO at LURE on the instrument previously described in [31]. Automatic sampling cycles including 30 s accumulation time for the instrumental response function and 90 s acquisition time for each polarized component were carried out such that a total number of $2–4\times10^6$ counts was reached in the fluorescence intensity decay. Analyses of the fluorescence intensity decays as sum of exponentials were performed by the maximum entropy method (MEM) [32,33]. Analyses of the polarized fluorescence decays were performed by using the associated model of the anisotropy, associating all lifetimes to each rotational motion, were performed by MEM [34].

3. Results

3.1. Crystal structure of the D226K Anx5 mutant

The side-chain of the mutated lysine residue K226 was clearly defined in the electron density map (Fig. 2), confirming the mutation. The crystallization conditions used for the preparation of the D226K mutant crystal, i.e. less than 10 mM calcium, were those usually leading to the buried conformation of the IIIA–IIIB loop for wild-type annexin V (A-form)

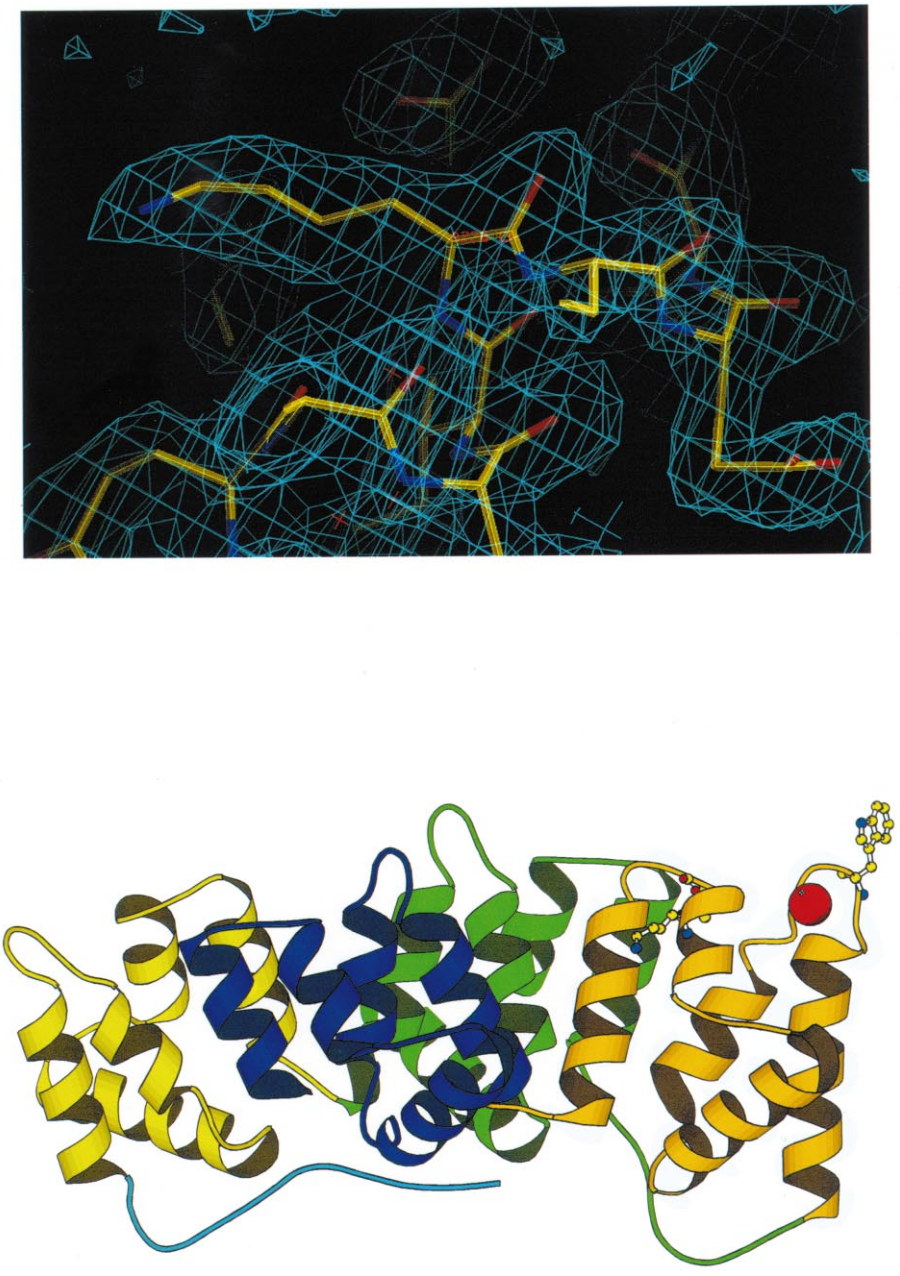

Fig. 2. Upper panel: Electron density ($3F_o-2F_c$) map contoured at 1σ of the region around K226. Lower panel: Ribbon representation of the structure of domain III in the D226K mutant of annexin V. K226 and T229 side-chains are represented. Figure made using Molscript [48].

[15]. Yet in the final model of the structure of the D226K mutant we find the IIIA–IIIB loop exposed on the surface of the molecule, with the calcium-binding site formed and 100% occupied (Fig. 2). Similarly to the 'open' wild-type structures, a sulfate ion was found bound to the calcium ion (the occupancy factor of the sulfate ion is 80%). Overall, the conformations of domain III of the mutant and of the isomorphous wild-type structures are very close (root-mean-square difference of backbone atoms is 0.53 Å).

The only difference between the wild-type and mutant structures in the occupancy of the calcium-binding sites in the other three domains. Besides the principal calcium site of domain III, we did not find any other principal or secondary calcium-binding sites occupied in the mutant structure. The absence of calcium ions is reflected in the higher mobility of calcium-binding loops in the three domains compared to the calcium-saturated form [15], as seen from the rather disordered electron density and the high B-factors of the residues of the AB-loop extremities in these domains.

3.2. The conformation of domain III in the D226K Anx5 mutant in solution: steady-state and time-resolved fluorescence intensity of W187

The D226K mutation induces a red-shift of the steady-state fluorescence emission spectrum of W187, from 325 nm in the wild-type to 338 nm (Fig. 3). This value of the emission maximum is similar to that of the wild-type Anx5 in the presence of 10 mM calcium concentration or at pH 4 in the absence of calcium [18,19]. Visual observation of the time-resolved fluorescence decays at neutral pH of the wild-type and of the D226K mutant protein shows strong changes (Fig. 4). The fluorescence decay of W187 in the D226K mutant is much slower than that in the wild-type in the absence of Ca^{2+}. Three excited state lifetime populations are observed for the mutant as for the wild-type protein, but the lifetime values as well as their respective proportions are modified (Fig. 5A,B). The decay heterogeneity arises likely from the existence of rotamer inter-conversion at slow rates with respect to the fluorescence time-scale according to the classical rotamer model [35–40]. A long lifetime dominates the fluorescence decay of W187 in the D226K mutant, corresponding to a conformer

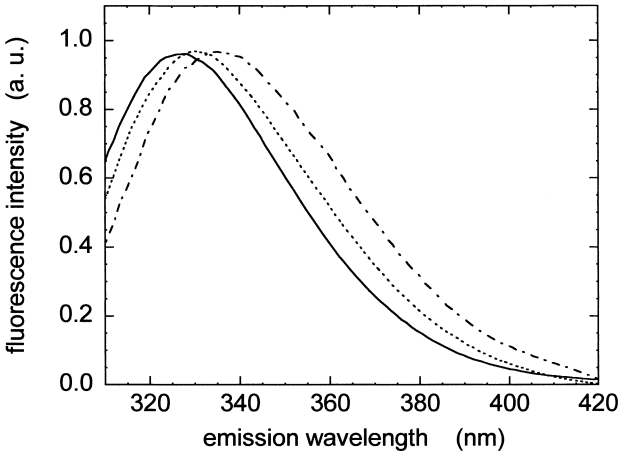

Fig. 3. Normalized steady-state fluorescence emission spectra of annexin V wild-type (—), of the D226K mutant (-·-) and of the T224V mutant (...). Excitation wavelength 295 nm.

without quenching contacts with the protein matrix, in a similar manner as the wild-type either in the presence of 10 mM calcium or at pH 4 [18]. This is in agreement with the expected solvent-exposed location of the indole ring, as seen in the crystal structure.

3.3. Accessibility of W187 to the solvent in the D226K mutant

The linear Stern–Volmer plots of the time-resolved acrylamide quenching for the mean excited state lifetime gives a value of the Stern–Volmer quenching constant K_{sv} of 2.69 M^{-1}, corresponding to a bimolecular quenching constant value k_q value of 1.3×10^9 M^{-1} s^{-1}. This value is three times higher than that measured for annexin V wild-type at neutral pH (4×10^8 M^{-1} s^{-1}) [18] but close to those measured for the wild-type either at pH 4 in the absence of calcium ($k_q = 1.4\times10^9$ M^{-1} s^{-1}) or at neutral pH in the presence of 10 mM calcium concentration (1.7×10^9 M^{-1} s^{-1}). Therefore, the accessibility of W187 to the solvent is higher in the D226K Anx5 mutant ($\sim$20–30%) than in the wild-type at pH 7 in the absence of calcium ($<10\%$). These estimations are performed relatively to *N*-acetyl tryptophanamide in water ($k_q = 6\times10^9$ M^{-1} s^{-1} [41]).

3.4. The dynamics of domain III in the D226K mutant: time-resolved fluorescence anisotropy decay

The visual observation of the experimental fluorescence anisotropy decay of the Anx5 D226K mutant shows a fast initial decrease, more pronounced than in the wild-type protein, followed by a slower part (Fig. 4). The analysis of the polarized fluorescence decays by the associated model of the anisotropy allows detecting two rotational correlation times (Table 2). The first one displays a value in the nanosecond time range which describes the local motion of the W187 residue. The value of the second one is close to that expected for the Brownian rotational correlation time of the protein (Table 2) [13,16,18]. The initial anisotropy value $A_{t=0}$ is nevertheless lower than expected for an immobilized tryptophan residue excited at 295 nm ($A_0 = 0.2$) [42]. This can be due to the presence of fast motions immeasurable with the time resolution of the instrumentation. A value of 26° for the semi-angle of the subnanosecond wobbling-in-cone motion can be calculated [43], larger than that observed for the Anx5 wild-type.

3.5. The effect of pH and Ca^{2+} on the conformation and dynamics of the D226K mutant

Decreasing the pH to 4 led to a large spectral red-shift by around 13–15 nm of the W187 fluorescence emission spectrum in the wild-type protein [18,19]. The strong implication of the D226 residue in this pH-induced red-shift is demonstrated by the observation that only a small 3-nm red-shift of the steady-state fluorescence emission spectrum of the D226K mutant is observed by reducing the pH to 4: most of the red-shift is already achieved by the D226K mutation. The excited state lifetime profile remains almost unchanged as a function of pH (Fig. 5C), confirming that the local environment of W187 is not affected by mild-acidic pH treatment of the D226K mutant. The fluorescence anisotropy decays monotonously to a plateau value (not shown). The analysis with the one-dimensional model shows an initial nanosecond decay followed by an infinite anisotropy value, which indicates that aggregation of the protein takes place in mild-acidic pH conditions as for the wild-type [18]. The amplitude of the local motion does not

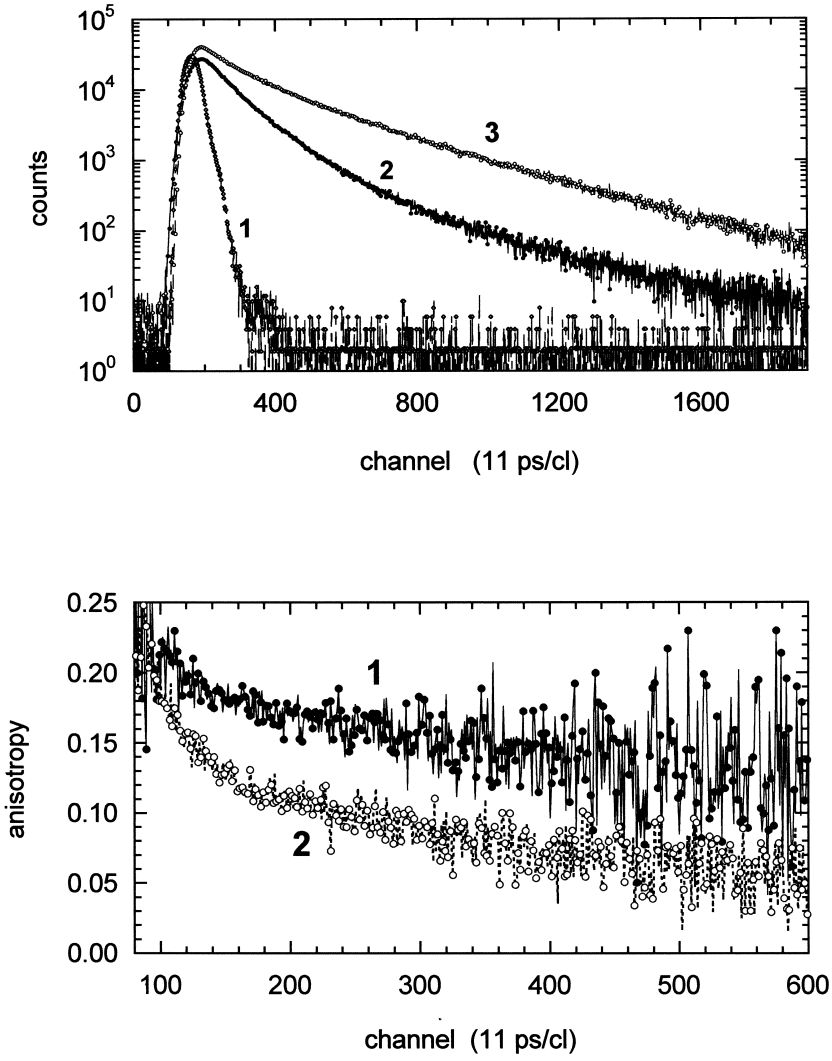

Fig. 4. Upper panel: Experimental fluorescence intensity decays of W187 reconstructed from the polarized decays $I_{vv}(t)$ and $I_{vh}(t)$ such as: $I(t) = I_{vv}(t)+2\beta_{corr}I_{vh}(t)$. Curve 1: instrumental response function; curve 2: fluorescence intensity decay of Anx5 wild-type and curve 3: fluorescence intensity decay of Anx5 D226K mutant at pH 7. Lower panel: Experimental fluorescence anisotropy decay $A(t)$ of W187 in Anx5 reconstructed from the polarized decays $I_{vv}(t)$ and $I_{vh}(t)$ such as: $A(t) = (I_{vv}(t)-\beta_{corr}I_{vh}(t)/I_{vv}(t)+2\ \beta I_{vh}(t)$. β_{corr} is a correction factor accounting for the difference in transmission of the $I_{vv}(t)$ and $I_{vh}(t)$ components of the optics [49]. Curve 1: Anx5 wild-type; curve 2: Anx5 D226K mutant.

change significantly as compared to that at neutral pH (Table 2).

In contrast to mild-acidic pH, Ca^{2+} affects the conformation of domain III. The presence of 10 mM calcium further shifts to the red (from 338 to 345 nm) the steady-state fluorescence emission spectrum of the D226K mutant. The excited state lifetime profile is also changed: a significant increase of the long lifetime amplitude by 40% is observed. This shows that the W187 rotamer without quenching contact with protein moieties is favored by Ca^{2+} binding, like for Anx5 wild-type [16]. The W187 mobility is also increased, as shown by the value of the semi-angle of the wobbling-in-cone motion (Table 2).

3.6. The conformation of domain III in the T224V mutant

The T224V mutant was crystallized in the space group $P6_3$ with cell dimensions $a = b = 99.34$ Å, $c = 129.69$ Å, $\gamma = 120°$, but the diffraction was limited to 5 Å. These crystals are isomorphous to annexin V crystals of the A-form of the protein (W187 buried within the protein matrix) [22]. The fold of domain III could be followed in the electron density map, confirming the conformation of the A-form (data not shown).

In agreement with these observations, the steady-state fluorescence emission spectrum of W187 in the T224V mutant of Anx5 at neutral pH displays a maximum located at 328 nm (Fig. 3), only 3 nm more to the red than that of the wild-type. The lifetime distribution is similar to that of the wild-type [13,16,18], the proportion of the shortest lifetime is strongly increased compared to the wild-type, while the lifetime values are shorter (Fig. 5E). Acrylamide quenching experiments shows that the value of the bimolecular quenching constant is low ($k_q = 6.2\times10^8$ M^{-1} s^{-1}) and of the order of magnitude of that of the wild-type protein [13,18]. These data indicate that the W187 residue remains in a buried location but that the more mobile conformer is favored.

The anisotropy decay shows two rotational correlation time peaks, one corresponding to the Brownian rotation correlation time of the protein and a second peak at a shorter times

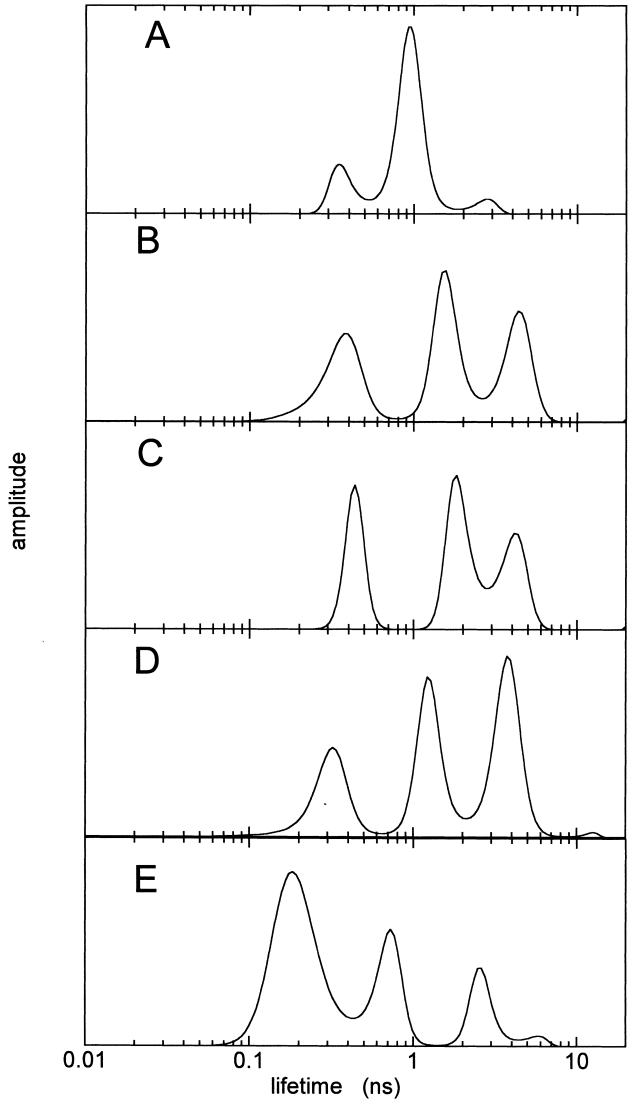

Fig. 5. Excited state lifetime distribution recovered by MEM of the fluorescence intensity decay W187 of annexin V. MEM analysis was performed on the fluorescence intensity $T(t)$ reconstructed from the parallel and perpendicular polarized components $I_{vv}(t)$ and $I_{vh}(t)$ such as $T(t) = I_{vv}(t) + 2\ \beta_{corr} I_{vh}(t) = \int_0^\infty \alpha(\tau)\exp(-t/\tau)\mathrm{d}\tau$. A: Wild-type pH 7 (emission wavelength: 325 nm). B: D226K mutant pH 7 (emission wavelength: 340 nm). C: D226K mutant pH 7 with 10 mM $CaCl_2$ (emission wavelength: 340 nm). D: D226K mutant pH 4 (emission wavelength: 340 nm). E: T224A mutant pH 7.

describing the W187 internal rotation (Table 2). The value of the semi-angle of the wobbling-in-cone subnanosecond motion is slightly larger than that of the Anx5 wild-type.

4. Conclusion

The Ca^{2+}-induced large-scale conformational change of Anx5 involves a concerted motion of two loops connecting helices IIIA–IIIB and IIID–IIIE respectively, which moves the E228 residue, which coordinates the Ca^{2+} ion, by ~12 Å and leads to the exposure of thw W187 residue on the protein surface (Fig. 1). Recent computer simulations of the pathway of this large conformational change revealed its complexity and the large number of interactions that are altered along the reaction path of the transition [21]. The analysis of this pathway emphasizes the important role of a few acidic amino acid residues in the conformational change, amongst them obviously E228 mentioned above and D226. These residues undergo main-chain transitions during the pathway. The particularity of D226 is illustrated in the simulation by the fact that it interacts transiently with the W187 indole ring in the 'saddle-point' (highest energy point) of the transition pathway, and blocks the W187 movement in/out of the protein cavity [21]. In the 'closed' A-form of domain III, it participates in a hydrogen-bond interaction with the hydroxyl group of the T229 side-chain (Fig. 1). Its important role in the conformational transition, suggested by the simulation and by the three-dimensional structure, is experimentally underlined in the present work. The point mutation of the D226 residue is sufficient to provoke the transition of domain III from the 'closed' A-form to the 'open' B-form. In the three-dimensional structure of Anx3, which possesses a lysine residue in position equivalent to 226 (K229), domain III, which contains a Trp residue in the IIIA–IIIB loop at an equivalent position as in Anx5 (W190), remains in the 'open' B-form even in the absence of Ca^{2+}, with the W190 residue exposed to the solvent [23]. This observation in fact directed our choice in performing the mutation. The presence of a positive instead of a negative charge may also lead to the existence of repulsive interactions, which could destabilize the A-form. The absence of any pH-induced conformational change in the Anx5 D226K mutant provides strong support for the crucial role of D226 in the transition. Nevertheless, we observe that Ca^{2+} in the mM concentration range provokes a further red-shift of the fluorescence emission spectrum of W187 in the mutant, suggesting that the formation of the Ca^{2+}-binding site is not totally achieved in the mutant in the absence of Ca^{2+}.

In conclusion, an increasing number of reports shows that

Table 2
Time-resolved anisotropy decay parameters of the W187 fluorescence emission in the annexin V D226K and T224V mutants obtained by MEM using the one-dimensional model

Sample	θ_1 (ns) (β_1)	θ_2 (ns) (β_2)	$A_{t=0}$	ω_{max} (°)
Wild-type	–	14.5 ± 0.5 (0.180 ± 0.004)	0.180 ± 0.004	14 ± 4
D226K pH 7	2.6 ± 0.8 (0.016 ± 0.009)	12.6 ± 1.8 (0.128 ± 0.026)	0.144 ± 0.017	26 ± 5
D226K pH 4	6.5 (0.047)	∞ (0.087)	0.134	29
D226K 10 mM $CaCl_2$ pH 7	1.2 (0.026)	8.5 (0.068)	0.094	46
T224-V pH 7	1.7 (0.023)	16.3 (0.141)	0.164	21

The fluorescence anisotropy is described by a sum of exponentials: $A(t) = \Sigma_i\ \beta_i\ \exp(-t/\theta_i)$ with $A_{t=0} = \Sigma_i\ \beta_i$. θ_i are the values of the rotational correlation times. A value of the intrinsic anisotropy A_0 of 0.2 was used for the calculation of the wobbling-in-cone angle ω_{max} according to: $A_{t=0}/A_0 = [1/2\ \cos\omega_{max}(1+\cos\omega_{max})]^2$ [43]. Error bars for three–six measurements are given for two series of experiments. They are representative of all the measurements.

pH plays an important role in the structure and dynamics of annexins, in addition to their sensitivity to Ca^{2+} [4,18, 19,44,45]. The increase in proton activity, which takes place at the membrane/water interface [46], could regulate their interaction with membranes and therefore partly explain the large-scale conformational change of domain III of Anx5 upon interaction with negatively charged membranes. The present report emphasizes the role of a specific acidic amino acid side-chain which acts as a molecular switch in this conformational change.

Acknowledgements: The technical staff of LURE is acknowledged for running the synchrotron ring during the beam sessions. This work has been supported in part by a Grant from EC (No. ERB-BIO4CT960083). Partial financial supports from CNRS, CEA, MESRT and INSERM are acknowledged.

References

[1] Gerke, V. and Moss, S.E. (1997) Biochim. Biophys. Acta 1357, 129–154.
[2] Swairjo, M.A. and Seaton, B.A. (1994) Annu. Rev. Biophys. Biomol. Struct. 23, 193–213.
[3] Raynal, P. and Pollard, H.B. (1994) Biochim. Biophys. Acta 1197, 63–93.
[4] Kubista, H., Hawkins, T.E., Patel, D.R., Haigler, H.T. and Moss, S.E. (1999) Curr. Biol. 9, 1403–1406.
[5] Meers, P. (1996) in: Annexins: Molecular Structure to Cellular Functions (Seaton, B.A., Ed.), Chapman and Hall, New York.
[6] Meers, P. and Mealy, T. (1993) Biochemistry 32, 5411–5418.
[7] Meers, P. and Mealy, T. (1993) Biochemistry 32, 11711–11721.
[8] Meers, P. and Mealy, T. (1994) Biochemistry 33, 5829–5837.
[9] Sopkova, J. (1994) Ph.D. Université de Paris-Sud, Orsay.
[10] Follenius-Wund, A., Piémont, E., Freyssinet, J.M., Gérard, D. and Pigault, C. (1997) Biochem. Biophys. Res. Commun. 234, 111–116.
[11] Silvestro, L. and Axelsen, P.H. (1999) Biochemistry 38, 113–121.
[12] Wu, F., Flach, C.R., Seaton, B.A., Mealy, T.R. and Mendelsohn, R. (1999) Biochemistry 38, 792–799.
[13] Sopkova, J., Vincent, M., Takahashi, M., Lewit-Bentley, A. and Gallay, J. (1999) Biochemistry 38, 5447–5458.
[14] Concha, N.O., Head, J.F., Kaetzel, M.A., Dedman, J.R. and Seaton, B.A. (1993) Science 261, 1321–1324.
[15] Sopkova, J., Renouard, M. and Lewit-Bentley, A. (1993) J. Mol. Biol. 234, 816–825.
[16] Sopkova, J., Gallay, J., Vincent, M., Pancoska, P. and Lewit-Bentley, A. (1994) Biochemistry 33, 4490–4499.
[17] Pigault, C., Follenius-Wund, A. and Chabbert, M. (1999) Biochem. Biophys. Res. Commun. 254, 484–489.
[18] Sopkova, J., Vincent, M., Takahashi, M., Lewit-Bentley, A. and Gallay, J. (1998) Biochemistry 37, 11962–11970.
[19] Beermann, B.B., Hinz, H.J., Hofmann, A. and Huber, R. (1998) FEBS Lett. 423, 265–269.
[20] Menger, F.M. and Mataga, K. (1979) J. Am. Chem. Soc. 101, 6731–6734.
[21] Sopkova-De Oliveira Santos, J., Fischer, S., Guilbert, C., Lewit-Bentley, A. and Smith, J.C. (2000) Biochemistry 39, 14065–14074.
[22] Huber, R., Römisch, J. and Paques, E.P. (1990) EMBO J. 9, 3867–3874.
[23] Favier-Perron, B., Lewit-Bentley, A. and Russo-Marie, F. (1996) Biochemistry 35, 1740–1744.
[24] Maurer-Fogy, I., Reutelingsperger, C.P., Pieters, J., Bodo, G., Stratowa, C. and Hauptmann, R. (1988) Eur. J. Biochem. 174, 585–592.
[25] Berendes, R., Voges, D., Demange, P., Huber, R. and Burger, A. (1993) Science 262, 427–430.
[26] Brick, P. (1994) Acta Cryst. D 50, 760–763.
[27] Lamzin, V.S. and Wilson, K.S. (1993) Acta Cryst. D 49, 129–147.
[28] Jones, T.A., Zou, J.Y., Cowan, S.W. and Kjeldgaard, M. (1991) Acta Cryst. A 47, 110–119.
[29] Murshudov, G. and Vagin, A.-A. (1997) Acta Cryst. D 53, 240–255.
[30] Rouvière, N., Vincent, M., Craescu, C.T. and Gallay, J. (1997) Biochemistry 36, 7339–7352.
[31] Vincent, M., Rouvière, N. and Gallay, J. (2000) Cell. Mol. Biol. 46, 1113–1131.
[32] Brochon, J.-C. (1994) Methods Enzymol. 240, 262–311.
[33] Vincent, M., Brochon, J.C., Merola, F., Jordi, W. and Gallay, J. (1988) Biochemistry 27, 8752–8761.
[34] Vincent, M. and Gallay, J. (1991) Eur. Biophys. J. 20, 183–191.
[35] Szabo, A.G. and Rayner, D.M. (1980) J. Am. Chem. Soc. 102, 554–563.
[36] Chang, M.C., Petrich, J.W., McDonald, D.B. and Fleming, G.R. (1983) J. Am. Chem. Soc. 105, 3819–3824.
[37] Petrich, J.W., Chang, M.C., McDonald, D.B. and Fleming, G.R. (1983) J. Am. Chem. Soc. 105, 3824–3832.
[38] Chen, R.F., Knutson, J.R., Ziffer, H. and Porter, D. (1991) Biochemistry 30, 5184–5195.
[39] Ross, J.B., Wyssbrod, H.R., Porter, R.A., Schwartz, G.P., Michaels, C.A. and Laws, W.R. (1992) Biochemistry 31, 1585–1594.
[40] Willis, K.J., Neugebauer, W., Sikorska, M. and Szabo, A.G. (1994) Biophys. J. 66, 1623–1630.
[41] Eftink, M.R. (1991) in: Topics in Fluorescence Spectroscopy, Vol. 2 (Lakowicz, J.R., Ed.), pp. 53–126, Plenum, New York.
[42] Valeur, B. and Weber, G. (1977) Photochem. Photobiol. 25, 441–444.
[43] Kinosita, K.J., Kawato, S. and Ikegami, A. (1977) Biophys. J. 20, 289–305.
[44] Langen, R., Isas, J.M., Hubbell, W.L. and Haigler, H.T. (1998) Proc. Natl. Acad. Sci. USA 95, 14060–14065.
[45] Isas, J.M., Cartailler, J.P., Sokolov, Y., Patel, D.R., Langen, R., Luecke, H., Hall, J.E. and Haigler, H.T. (2000) Biochemistry 39, 3015–3022.
[46] Teissie, J., Prats, M., Soucaille, P. and Tocanne, J.F. (1985) Proc. Natl. Acad. Sci. USA 82, 3217–3221.
[47] Brünger, A. (1992) Nature 355, 472–474.
[48] Kraulis, P.J. (1991) J. Appl. Crystallogr. 24, 946–950.
[49] Wahl, P. (1979) Biophys. Chem. 10, 91–104.